

## Structural, electronic, and magnetic properties of Au/Cr/Au(001) sandwiches: Theoretical total-energy studies

C. L. Fu and A. J. Freeman

*Department of Physics and Astronomy, Northwestern University, Evanston, Illinois 60201*

(Received 17 June 1985)

All-electron total-energy local-density studies of the structural, electronic, and magnetic properties of ordered Au/Cr/Au(001) sandwiches were undertaken to understand the report of superconductivity and the induced structural modification of Cr(001) by Au overlayers by Brodsky *et al.* These self-consistent spin-polarized calculations were carried out using the all-electron full-potential linearized-augmented-plane-wave method. Predicted structural properties, magnetic properties, charge and spin densities, contact hyperfine fields, and single-particle spectra are presented and discussed. The Cr lattice is found to be the same as in its bulk bcc environment. The Au-Cr interlayer spacing is expanded by about 3% with respect to the average of the bulk Au fcc and Cr bcc spacings; this expansion is mostly due to the formation of magnetic order at the interface. An enhancement of the Cr magnetic moment at the interface (to  $1.55\mu_B$ ) is predicted, which while  $0.94\mu_B$  less than that found for the surface layer in Cr(001), indicates the persistence of Cr surface states near  $E_F$  at the interface with the Au overlayers. These surface states, however, become more delocalized by their hybridization with the low-lying Au  $d$  band. Both the bcc structure of Cr layers and the magnetic character of the interface Cr states argue against models proposed previously for the occurrence of superconductivity. We conclude that superconductivity is not a property for ordered Au/Cr/Au(001) sandwiches but that disorder may play some role.

### I. INTRODUCTION

Recent progress in the fabrication and property modifications of artificial materials, such as thin films, sandwiches, and modulated structures, has generated a great deal of interest. The excitement surrounding this development lies in the possible discovery and synthesis of new materials with desired properties designed to specification, which may permit new phenomena to be investigated and novel devices to be made. Concurrently, advances in computational-theoretical approaches have made precise results and successful predictions possible.<sup>1</sup> In coordination with experimental studies, these theoretical efforts have led to the appearance of new and quite unexpected phenomena, and clues to understanding them. Thus, for example, considerable interest exists in the Cr(001)/Au(001) system because (i) the report of superconductivity in Au/CrAu(001) sandwiches [ $\sim 25$  Å multilayers of Cr sandwiched by thick Au(001) films] by Brodsky *et al.*<sup>2</sup> with a transition temperature up to 3 K, (ii) a close to perfect epitaxial growth due to a nearly perfect match of the two-dimensional (2D) lattice translational vectors for Au(001) and Cr(001) at the interface, and (iii) the intriguing magnetic properties of both bulk and surface Cr,<sup>3</sup> which are related to the dramatic difference between the bulk and surface electronic structures, offer exciting opportunities for investigating their interface electronic states and related physical properties. [For the Cr(001) surface, an induced ferromagnetism in its surface layer with an associated magnetic moment of  $2.49\mu_B$  concurrent with antiferromagnetic coupling in the bulk has been observed<sup>3</sup> in recent angle-resolved photoemission ex-

periments and predicted theoretically<sup>4</sup> in an independent study.]

The remarkable aspect of the reported existence of superconductivity in Cr, which is expected to be related to the existence of a high density of states (DOS) at  $E_F$ , or  $N(E_F)$ , is that for bulk bcc antiferromagnetic Cr,  $E_F$  is located in the deep valley separating bonding and antibonding DOS peaks. For this reason, Brodsky *et al.*<sup>2</sup> proposed that thick Au layers would cause a structural modification of Cr to the fcc lattice, and that superconductivity would follow from the formation of metastable fcc Cr when sandwiched by fcc Au. This proposal was supported by electronic energy-band calculations<sup>5</sup> for bulk fcc Cr, where a high  $N(E_F)$  was found. Moreover, recent x-ray diffraction experiments<sup>6</sup> performed on Au/Cr/Au(001) sandwiches appear to confirm that the fcc phase forms a major fraction of the epitaxial Cr domain. However, several other experiments, namely, the analyses of extended x-ray adsorption fine structure (EXAFS) in the same study<sup>6</sup> and low-energy electron-diffraction (LEED) and photoemission studies of Cr on Au(001) by Zajac *et al.*<sup>7</sup> reveal that the Cr atoms are in a bcc environment.

The hypothesis that fcc Cr leads to superconductivity is based on the structural and electronic properties of the bulk lattice. However, there is another well-known structural-geometrical related electronic mechanism that is able to give rise to high  $N(E_F)$  in the middle of the  $d$  band for transition metals, namely, the reduction of local symmetry and atomic coordination such as occurs at the surface of a metal. In fact, this high surface DOS at  $E_F$  is directly related to several observed phenomena at (001) surfaces, notably, structural phase transitions<sup>8</sup> (in  $4d$  and

5d transition metals such as Mo and W) and surface-induced enhancement of ferromagnetism<sup>3</sup> (3d transition metals such as Cr, Fe, and Ni). In the case of a transition-metal–noble-metal interface, the expectation is that the effect of the noble-metal overlayers is to delocalize the surface states of the transition metals. It turns out, however, that the basic features of the surface electronic states are retained at the interface due to the dissimilarity of their respective electronic structures (and less than expected hybridization). This electronic behavior has been demonstrated previously at the Ag/Fe(001) interface.<sup>9</sup> For Au/Cr(001), the same expectation of the persistence of surface states at the interface should remain—as verified theoretically from the band calculations of a Au overlayer on top of four-layer Cr(001) by Feibelman and Hamann.<sup>10</sup> On the basis of their investigation, which was limited to the paramagnetic state, these authors proposed that the  $N(E_F)$  arising from the interface states of Cr is responsible for the superconductivity. It should be emphasized that the surface layer of Cr(001) is ferromagnetic,<sup>3,4</sup> and the effect of nonmagnetic noble-metal overlayers may not always act to quench the magnetism [as, for example, in Ag/Fe(001)<sup>9</sup>]. In fact, recent photoemission measurements<sup>7</sup> on Cr as an overlayer on Au confirms that the magnetic ordering of the Cr layer persists at the interface. As a consequence, there are obvious difficulties in attributing the superconductivity to interface electronic states. On the other hand, it becomes even more interesting to further explore possible metastable structural properties as well as the electronic and magnetic properties of the Au/Cr(001) interface, since the dilemma remains regarding bcc versus fcc structures and superconductivity versus magnetism.

In this paper, we present results of a highly precise self-consistent, all-electron total-energy full-potential linearized-augmented-plane-wave (FLAPW) local-spin-density-functional study of the structural, electronic, and magnetic properties of Au/Cr/Au(001) slabs. In Sec. II the calculation model and theoretical approach are briefly described. Results on the structural properties (the interlayer spacings of Cr-Cr, Cr-Au, and Au-Au layers), charge density, magnetic moment, and spin density, including the contact hyperfine interaction, are presented in Sec. III and compared with the corresponding results obtained for the clean Cr(001) surface. The one-particle energy spectra are discussed in Sec. IV with particular regard to the role played by the interface states of Cr in the occurrence of interface magnetism. Finally, the relevance of this work to the reported superconductivity is also discussed.

## II. CALCULATIONAL MODEL

The remarkable feature about the Cr/Au(001) structure is the almost exact matching in surface translation vectors which makes it possible to grow samples with only a very small lattice strain<sup>2</sup> (0.02%). This is shown schematically in Fig. 1(a) for fcc Au and bcc Cr, with the (001) plane of Au(001) rotated by 45° with respect to that of Cr(001); in this arrangement there is an almost exact matching of their primitive 2D square nets because the experimental lattice constant of Cr (2.88 Å) is almost exactly a factor of

$\sqrt{2}$  smaller than that of Au (4.08 Å). As is seen from Fig. 1(a), the resulting stacking has atoms in the fourfold hollow site of adjacent atomic-layer planes. As mentioned earlier in Sec. I, superconductivity in the Cr/Au sandwiches has been attributed to a change in the Cr structure from bcc to fcc. As is clear from Fig. 1(a), to produce a fcc Cr layer structure by sandwiching with Au would require an expansion of the Cr interlayer spacing by exactly a factor of  $\sqrt{2}$ . In this study, we adopt the geometrical structure shown in Fig. 1. The Au/Cr/Au(001) sandwich is represented by a single slab consisting of seven atom layers—two layers of Au(001) on either side of a three-layer Cr(001) film [cf. Fig. 1(b)]. The number of Cr layers is extended to five for studying the effect of film size on the electronic and magnetic properties of Au/Cr/Au(001) sandwiches. The interlayer spacings are determined using the FLAPW total-energy approach<sup>11</sup> by treating the Cr-Cr, Cr-Au, and Au-Au layer spacings as independent variational quantities.

The local-density equations<sup>12</sup> are solved self-consistently by use of the FLAPW method.<sup>1</sup> In this method, no shape approximations are made to the poten-

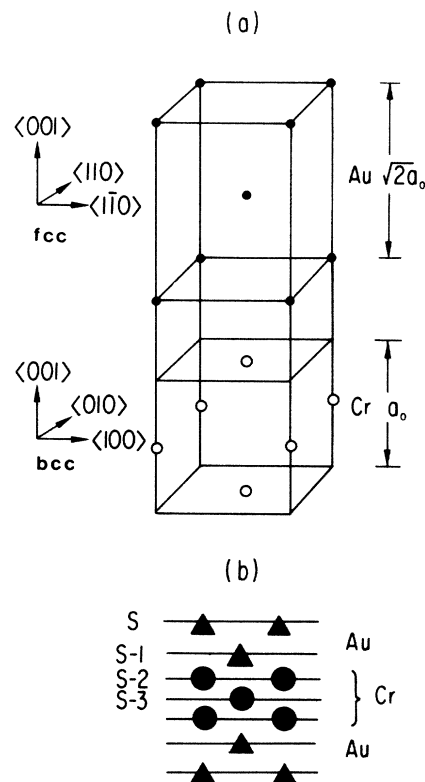


FIG. 1. (a) Schematic representation of an (001) interface of fcc Au with (001) bcc Cr. Note that the Au lattice constant (4.08 Å) is exactly a factor of  $\sqrt{2}$  larger than that of Cr (2.88 Å); the axis of Au is rotated by 45° with respect to that of Cr to form an exact matching of their primitive 2D square net. (b) Schematic geometrical structure of (110) planes of the Au/Cr/Au(001) sandwich employed in the present work, where Cr and Au atoms are represented by circles and triangles, respectively.

tial or charge density in solving Poisson's equation for a general potential<sup>13</sup> and all matrix elements corresponding to this general potential are rigorously taken into account in all parts of space. In addition, we treat the spherical cores fully relativistically and the valence electrons are calculated semirelativistically.<sup>14</sup> For the spin-polarized studies we employ the explicit form of the von Barth and Hedin<sup>15</sup> exchange-correlation potential with the Hedin-Lundqvist<sup>16</sup> potential for the paramagnetic case.

A total number of 550 augmented plane waves are used as a variational basis set, split into two blocks of about 275 basis functions, each using the mirror-plane reflection symmetry with respect to the center layer of the slab ( $z$  reflection). Within the muffin-tin (MT) spheres [with radius chosen to be equal to  $(\sqrt{3}/4)a$ ], the charge density and potential are expanded into a lattice harmonic with angular momentum components  $l \leq 8$ . A total number of 28  $k$  points in the irreducible wedge of the 2D Brillouin zone is used to converge the total energy and spin density. Self-consistency is assumed when the root-mean-square difference between the input and output charge densities and spin densities is less than  $3 \times 10^{-4} e/(a.u.)^3$ .

### III. RESULTS

#### A. Structural properties

This section concerns the change of the interlayer spacings near the Au/Cr interface from their respective bulk values. More specifically, we explore: (i) the possibility of long-range Au-Cr interactions causing the Cr lattice to be in the metastable fcc structure, i.e., volume stretching by 41%, and (ii) the value of the interlayer spacing at the Au/Cr interface. For a seven-layer Au/Cr(3- $L$ )/Au film depicted in Fig. 1(b), we have three independent structural variables, the Au-Au, Cr-Cr, and Au-Cr interlayer spacings. As a first step in examining the Cr and Au lattice structure, we calculated the total energy of the system for different combinations of bulk bcc and fcc interlayer spacings for these three quantities. The results are summarized in Table I, where possible configurations are listed in order of decreasing total energy. Apparently, just one layer away from the Au/Cr interface, bulk Cr (bcc) and Au(fcc) structures are retained; this indicates that metallic screening lengths induced by the interface are of the order of the interlayer distance. Next, to be more precise, total-energy calculations were performed as

TABLE I. Total energies (in Ry) for different combinations of bulk bcc or fcc spacings for Au-Au, Cr-Cr, and Au-Cr interlayer distances in a Au/Cr(3- $L$ )/Au(001) sandwich.

Au-Au	Interlayer spacing		$E_T$ (Ry)
	Cr-Cr	Au-Cr	
bcc	bcc	bcc	-158 590.534
fcc	fcc	fcc	-158 590.626
fcc	bcc	bcc	-158 590.762
fcc	bcc	fcc	-158 590.817
fcc	bcc	$\frac{\text{fcc} + \text{bcc}}{2}$	-158 590.843

a function of the Au-Cr interlayer distance with Cr and Au kept at their respective bulk structures. For the paramagnetic state, the results are shown by the solid curve in Fig. 2. The total-energy curve shows an asymmetric form with a higher energy close to the bcc side, which reflects the outward pressure experienced by the Au  $s,p$ -like electrons as the lattice is compressed. Furthermore, the minimum of the total energy occurs at a position (indicated by an arrow in Fig. 2) which is very close to an average of the bulk bcc and fcc spacings—a result long suspected by materials scientists. Finally, with the Au-Au and Au-Cr spacings held at their equilibrium values, total energies are compared for Cr-Cr (i) at its bcc value, and (ii) with a 5% expansion from its bulk interlayer spacing, in order to examine the possible expansion of the Cr lattice in the Au sandwich environment. We find that case (i) has a lower total energy (by 9 mRy per interlayer spacing). This result follows from the strong local screening effect at the interface and the weak hybridization between the Au and Cr  $d$  bands (discussed below) and thus fails to justify the volume expansion of the Cr lattice to the Au spacing as proposed previously<sup>2</sup> to account for the occurrence of superconductivity. Furthermore, this calculation clearly indicates the abruptness of the transition-metal-noble-metal interface, as confirmed by the experimental studies<sup>7</sup> of the epitaxy and electronic structure of  $p(1 \times 1)$  Cr/Au(001).

#### B. Magnetic properties

We have shown above that the Cr atoms near the interface tend to be in their metallic bcc lattice environment. In addition, we recall that (i) for the clean Cr(001) surface,

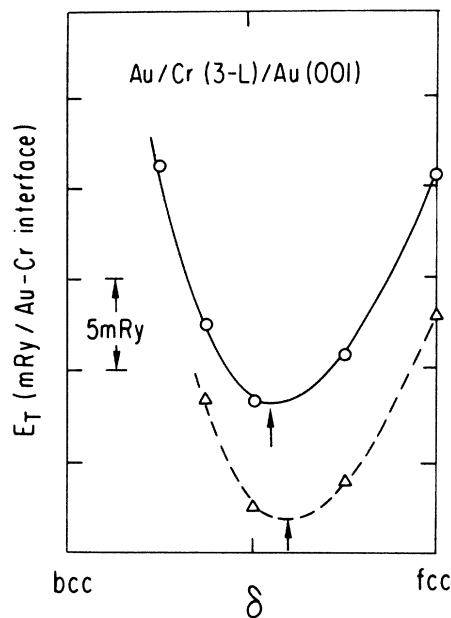


FIG. 2. Total energy as a function of Au-Cr interlayer spacing with Au and Cr at their respective bulk fcc and bcc lattice values for the seven-layer Au/Cr(3- $L$ )/Au(001) sandwich. Solid and dashed curves represent paramagnetic and spin-polarized states, respectively; arrows indicate the corresponding equilibrium Au-Cr lattice spacing.

there is a ferromagnetic ordering at the surface layer with a sizeable magnetic moment of  $2.5\mu_B$  per surface atom, and (ii) the interface states localized at the Cr site near  $E_F$  retain the same feature of the surface states for Cr(001) with Au overlayers on Cr(001), as found by Feibelman and Hamann<sup>10</sup> and in this investigation [for Cr(001), these surface states give rise to the surface ferromagnetic phase transition]. As a result, one would question whether the so-called "magnetic proximity effect," as being generally believed and observed to quench the magnetic ordering by nonmagnetic materials, would be equally applicable to this system. In this context it is also important to understand the reported superconductivity of multilayers of Cr(001) sandwiched by Au, owing to the exclusion of magnetism and superconductivity under ordinary circumstances. We therefore carried out additional spin-polarized calculations in order to investigate possible magnetic ordering near the interface.

Contrary to any so-called magnetic proximity effect, results based on the self-consistent calculations predict a significant enhancement of the Cr magnetic moment at the interface [to  $1.75\mu_B$ /atom at the Cr interface layer and  $-1.07\mu_B$  for the subinterface Cr layer in the Au/Cr(3-L)/Au sandwich] with respect to the Cr bulk value ( $0.59\mu_B$ ).<sup>17</sup> Furthermore, there is a sizeable induced polarization of  $0.06\mu_B$  on the interface Au site. It is obvious that a "bulklike" picture for Cr atoms at the Au/Cr interface is no longer applicable. Instead, a close resemblance of the Cr interface states near  $E_F$  to the Cr surface states is more appropriate from an electronic structure analysis (see below). In other words, although the presence of Au overlayers partially reimposes the bulk periodicity, the low-lying *d*-band states of the Au ensures that the surface states of Cr(001) near  $E_F$  are not strongly perturbed. As a result, the Stoner criterion for interface ferromagnetism is still fulfilled, and, while the effect of the Au overlayers is to decrease the magnetic moment by about  $0.9\mu_B$  and  $0.4\mu_B$  from the corresponding values of the three-layer Cr(001) film, the result still shows a substantial increase in the magnetic moment compared to bulk.

These results were obtained as reported for the Au-Cr interlayer spacing at the average of the bulk fcc and bcc spacings (i.e., calculated interlayer spacing for the paramagnetic state). The effect of the magnetic ordering on the total-energy and lattice spacing were further examined by means of total-energy spin-polarized calculations. The results are presented by the dashed curve in Fig. 2, which shows that (i) the inclusion of the spin-polarization expands the Au-Cr interlayer spacing by about 3%, and (ii) the total energy is lowered by 6 mRy (per interface) in favor of the formation of an ordered magnetic moment. In addition, we find that the effect of varying the Au-Cr lattice spacings on the magnetic moment is small: the magnetic moments increase to  $1.82\mu_B$  and  $-1.16\mu_B$  for interface and subinterface Cr atoms when the Au-Cr spacing is expanded to that of the fcc lattice and decrease to  $1.66\mu_B$  and  $-1.0\mu_B$  when the Au-Cr spacing is contracted by about 10% from its equilibrium value. These small effects again indicate the role played by the large separation in energy of the Cr and Au *d* bands.

The interface (surface) ferromagnetism of Cr(001) is closely related to the reduced dimensionality and lower symmetry for atoms near the interface (surface). In fact, for a monolayer Cr film sandwiched by Au(001), we predict a giant magnetic moment of  $3.10\mu_B$  induced onto the Cr site.<sup>18</sup> This behavior can again be understood from the electronic isolation of the 2D Cr monolayer. However, as reported above, the magnetic moment of this single-Cr-layer structure is substantially decreased with increasing number of Cr layers—but still leaves a net total moment of  $2.4\mu_B$  for the Au/Cr(3-L)/Au sandwich. Hence, one expects that the effect of additional Cr layers would possibly further reduce the magnetic moment of Cr layers. This expectation is borne out by the calculation on five layers of Cr(001) sandwiched by Au(001) (a total of nine layers in the film): the magnetic moment of the interface and subinterface Cr atoms decreases somewhat to  $1.55\mu_B$  and  $-0.77\mu_B$ , and a moment of  $0.67\mu_B$  is found on the Cr site at the center of the film (cf. Table I). Since the center layer value is close to the bulk value ( $0.59\mu_B$ ), this indicates that the screening length for the spin density induced by the interface is two atomic layers [which is similar to that for the clean Cr(001) surface]. Moreover, it ascertains that five layers of Cr can already give a good quantitative description of the electronic and magnetic properties of even thicker films when sandwiched by Au(001).

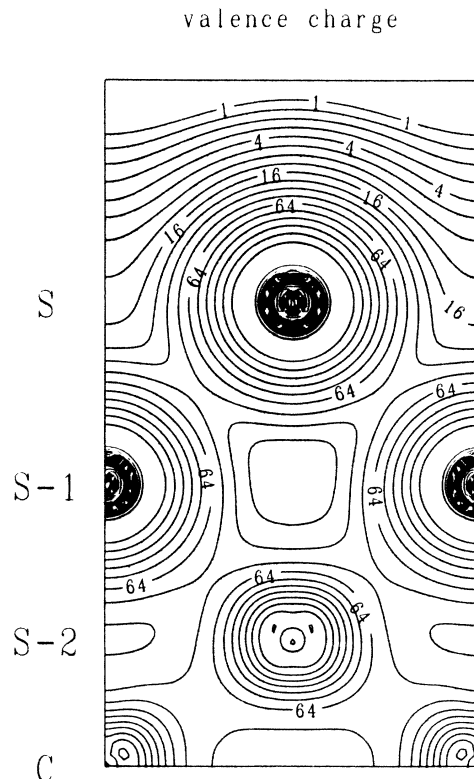


FIG. 3. Valence electronic charge density on the (110) plane for the seven-layer Au/Cr(3-L)/Au(001) sandwich in units of  $1 \times 10^{-3} e/(a.u.)^3$ . Adjacent contour lines differ by a factor of  $\sqrt{2}$ .

TABLE II. Theoretical work function (in eV) and layer-by-layer MT valence electron charge (in electrons) and magnetic moment (in  $\mu_B$ ) for Cr(001) slabs and Au/Cr/Au(001) sandwiches from the surface (*S*) to the center layer of the film.

	Au/Cr/Au		Cr(001)		
	Cr(3-L)	Cr(5-L)	Cr(3-L)	Cr(7-L)	
Charges in spheres					
<i>S</i> (Au)	8.95	8.95	<i>S</i> (Cr)	4.69	4.67
<i>S</i> -1 (Au)	9.06	9.06	<i>S</i> -1 (Cr)	4.95	4.95
<i>S</i> -2 (Cr)	4.83	4.83	<i>S</i> -2 (Cr)		4.95
<i>S</i> -3 (Cr)	4.95	4.95	<i>S</i> -3 (Cr)		4.95
<i>S</i> -4 (Cr)		4.95			
Moment					
<i>S</i>	0	0		2.70	2.49
<i>S</i> -1	0.07	0.06		-1.59	-1.29
<i>S</i> -2	1.75	1.52			0.89
<i>S</i> -3	-1.07	-0.77			-0.89
<i>S</i> -4		0.67			
(Bulk)		0.59			
Work function (eV)	5.57	5.65		4.25	4.05

The calculations clearly show that the high local density-of-states (or interface states) at  $E_F$  for Cr at the Au/Cr interface tends to favor magnetism, which is opposite to the mechanism reported for superconductivity by Feibelman and Hamann.<sup>10</sup>

### C. Charge density and spin density

In order to gain further insight into the formation of the interface, we list in Table II the calculated results for the layer-by-layer total charge density inside the MT spheres and a comparison with the corresponding results for clean Cr(001) films. As discussed previously, there is a decrease in the total charge density inside the sphere at the surface, due mainly to the loss of *p*-like charge into the vacuum region. At the interface, this amount of charge is partially recovered by the imposition of Au layers. Moreover, the charge density approaches the bulk values very rapidly, as is seen from the constancy of the charge within the Cr spheres just one atomic layer away from the interface (or surface). Figure 3 presents the charge-density map in the (110) plane of the upper half of the Au/Cr(3-L)/Au seven-layer film. It reveals that the charge density in the center Cr layer already exhibits the same contours as do those for the inner layers of a Cr(001) film. Furthermore, this short screening length induced by the interface is demonstrated in the calculated work function ( $5.60 \pm 0.05$  eV; cf Table II) for our film geometry (the Au surface layer is one layer away from the interface), which is in excellent agreement with the experimental work function of the Au(001) surface (5.57 eV).<sup>19</sup>

Figure 4 presents the corresponding spin density for the Au/Cr(3-L)/Au film. It exhibits antiferromagnetic coupling with appreciable spin polarization between adjacent Cr layers in the (001) direction and a relatively small induced positive spin density on the Au site at the interface. The layer-projected spin magnetic moments within each MT sphere are also summarized in Table II. Both

for Cr and Au, the contribution to the spin polarization is mainly due to the imbalance of the majority- and minority-spin *d*-like electrons within each MT sphere; the contribution from delocalized *s*- and *p*-like electrons is less than  $0.02\mu_B$ .

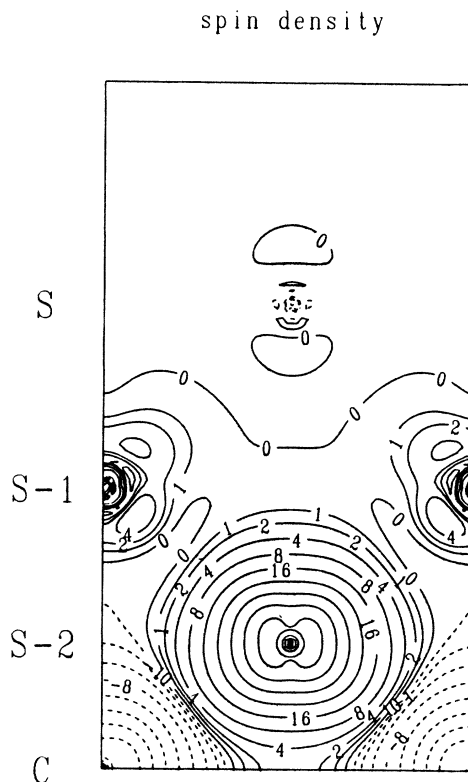


FIG. 4. Spin-density map on the (110) plane for the seven-layer Au/Cr(3-L)/Au(001) sandwich in units of  $1 \times 10^{-3} e/(a.u.)^3$ . Negative densities are indicated by dashed lines. Adjacent contour lines differ by a factor of 2.

TABLE III. Electronic spin densities at the nuclei in the three-layer Cr(001) film and Au/Cr(3-L)/Au(001) sandwich. The last column shows the ratio of the core spin density at the nucleus and the corresponding magnetic moment in the corresponding sphere.

	Hyperfine field (kG)			Moment ( $\mu_B$ )	$H_{cf}$ (core)/ $\mu_B$ (kG per unpaired spin)
	Core	Valence	Total		
Au/Cr(3-L)/Au					
$S$ (Au)	$\sim 0$	-2100	-2100	0	
$S-1$ (Au)	-320	-2400	-2700	0.07	
$S-2$ (Cr)	-220	98	-122	+1.75	-124
$S-3$ (Cr)	130	-160	-28	-1.07	-123
Cr(3-L)					
$S$ (Cr)	-352	279	-73	2.70	-130
$S-1$ (Cr)	199	-189	10	-1.59	-125

Consider now the spin density at the nucleus, which gives the Fermi contact hyperfine field ( $H_{cf}$ ). In an earlier study on Cr(001), we showed that (i) a three-layer film can already give essentially the same  $H_{cf}$  result for the surface layer as do thicker films, and (ii) finite film size effects on the valence contribution (from  $s$ -like electrons) to  $H_{cf}$  cannot be excluded from the calculation at the center of the film. We therefore will mainly concentrate on  $H_{cf}$  for atoms at the interface of a Au/Cr(3-L)/Au film. Table III summarizes the contact hyperfine field, conveniently decomposed into two components<sup>20</sup> (the negative polarization of core  $s$  electrons and the contribution from valence  $s$ -like electrons), for both clean and Au overlayer covered Cr(001). As expected, the core-polarization scales vary precisely with the corresponding magnetic moment ( $d$  moment) within each MT sphere, regardless of the metallic environment. However, in contrast to the reduction of the magnetic moment, there is an enhancement of  $H_{cf}$  for Cr atoms (-122 kG) at the interface compared to that of the surface layer of free Cr(001) (-73 kG). This could be understood in terms of the large decrease of the direct polarization of  $s$ -like conduction electrons from its value for a free-standing surface for Cr atoms to that at the interface (from 279 to 98 kG), due to the partial reimposition of bulk boundary conditions by Au overlayers. (At the free-standing surface, the  $s$  density is more atomiclike and hence contributes a large direct valence polarization to  $H_{cf}$ .) Therefore, similar to the results reported for Ag/Fe(001), the use of the standard model for bulk materials where  $H_{cf}$  scales with the local moment would lead to the wrong conclusion on the behavior of the magnetic moment localized at the interface. Also, we notice that the Au valence contribution is very large and negative, indicating a direct exchange coupling between the localized Cr moment at the interface and the Au  $s$ - $p$  electrons. This gives rise to a Ruderman-Kittel-Kasuya-Yosida (RKKY)-type interaction and yields a negative valence-electron-spin density at neighboring Au sites.

#### D. Single-particle spectra

The study of the density of states decomposed by layers and  $l$ -like components gives some basic understanding of the interface-related features and the mechanism of interface-induced enhancement of magnetism. In Fig. 5

we present the layer-projected local DOS (LDOS) for a seven-layer paramagnetic Au/Cr(3-L)/Au film. The subinterface, or central, layer Cr atoms ( $S-3$ ) already exhibit the bulklike feature of having  $E_F$  located in the DOS valley separating bonding and antibonding states; differences are seen, however, in the LDOS of interface Cr atoms ( $S-2$ )—band narrowing together with an enhancement of the LDOS at  $E_F$ . Although this behavior is less pronounced than at the clean Cr surface, the surface states that give rise to surface ferromagnetism in Cr(001) are still present at the interface (but are more delocalized). As a consequence, this high LDOS of interface Cr ( $S-2$ ) at  $E_F$  (2.5 states/eV atom) induces a Stoner instability [ $IN(E_F) \gg 1$ , where  $I$ , the exchange-correlation integral,  $\sim 0.70$  eV] and ferromagnetic spin ordering at the Au/Cr interface. The hybridization of the Au and Cr  $d$  bands can be seen from (i) the increase of Cr  $d$ -like weight just below  $E_F$  on the Au site ( $S-1$ ) and the loss of states between -3 and -5 eV compared to clean Cr, but (ii) an increase in  $d$ -like population below -5 eV for Cr atoms ( $S-2$ ). However, this hybridization effect is local, as seen from the LDOS one layer away from the interface—a bulklike and surfacelike feature for Cr( $S-3$ ) and Au( $S$ ) atoms, respectively.

Figure 6 shows the calculated energy dispersion of the spin-up (majority-spin) states of interface Cr atoms, and spin-down states in a seven-layer Au/Cr(3-L)/Au film along the high-symmetry directions of the 2D Brillouin zone. The energy bands are sorted out for clarity into states with odd (upper panel) and even (lower panel) parities with respect to 2D rotational symmetry. States with odd and even parities with respect to  $z$  reflection are represented by dotted and dashed lines, respectively. Interface states of Cr, shown by solid curve, are defined as having their charge densities localized by more than 50% in the interface layer. Note that the occupied interface-state bands have a predominantly majority-spin character. The localization of these surface-state bands near  $E_F$ , as well as their similarity with those of a clean Cr(001) surface, indicates the persistence of the surface states at the interface: note particularly, the upward dispersion of the energy band with localized  $d_{xz}$ ,  $d_{yz}$ , and  $d_{x^2-y^2}$  orbitals at the interface along the  $\bar{\Gamma}-\bar{\Sigma}-\bar{M}$  direction. However, it is also noted that a considerable loss of weight of surfacelike

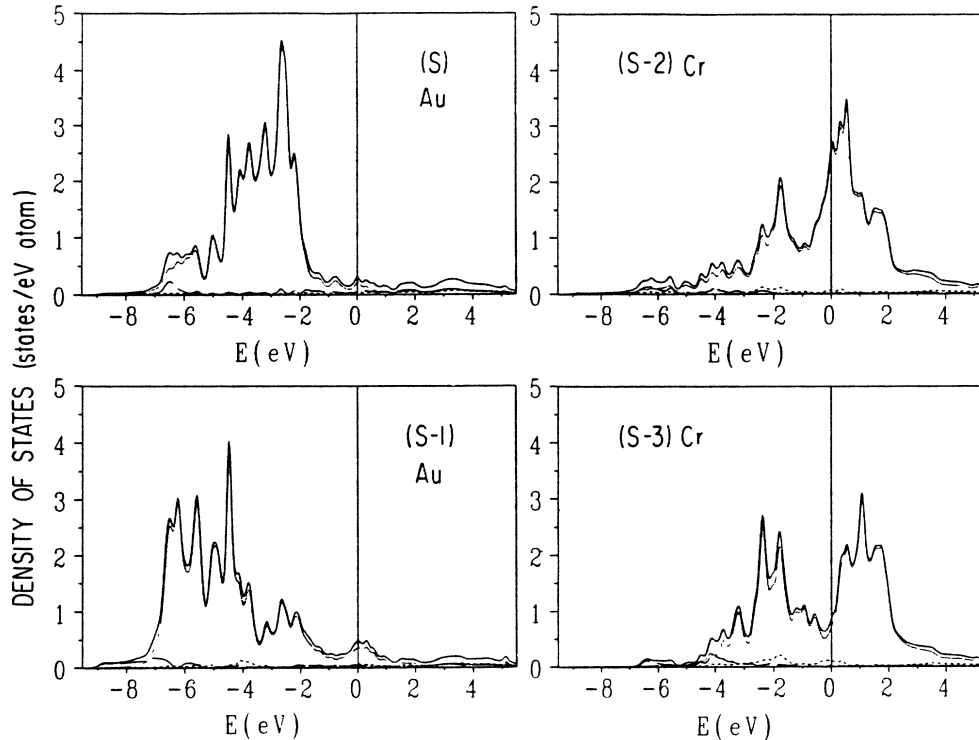


FIG. 5. Layer-projected and  $l$ -decomposed partial density of states in units of states/eV atom in the paramagnetic state of a seven-layer Au/Cr(3- $L$ )/Au(001) sandwich for the surface Au(S), interface Au(S-1), interface Cr(S-2), and subinterface Cr(S-3) layers.

character occurs for states with binding energy greater than 2.5 eV. This result is attributed to the hybridization with the Au  $d$  bands, which lie about 3–8 eV below  $E_F$ , as shown by the nearly degenerate even and odd partner (with respect to  $z$  reflection) of energy bands in Fig. 6. (The interaction between Au overlayers on either side of the film is prohibited by the presence of Cr layers in between.) With an increasing number of Cr layers, the  $d_{z^2}$ -like orbital near  $E_F$ , such as long  $\bar{\Gamma}\bar{X}$  direction, becomes more extended (and delocalized at the interface layer), which partially accounts for the slight reduction of the magnetic moment (by  $0.2\mu_B$ ) for thicker Cr films.

The  $l$ -decomposed partial LDOS in the interface and subinterface layer MT spheres of Cr are shown in Fig. 7 for the spin-polarized state. As expected, the LDOS are dominated by the  $d$  band and reveal a large spin-density imbalance. Comparing the results for the interface and subinterface layers shows the interface states to lie in the valley between bonding and antibonding bulklike peaks. The magnetic exchange splitting is found to be 1.3 eV for the interface states of Cr.

#### IV. DISCUSSION

One motivation of this investigation was to elucidate superconductivity (up to 3 K) of Au/Cr/Au(001) sandwich structures reported in Ref. 2. To date, two models have been applied to account for this behavior: (1) the existence of Au-Cr long-range interaction which changes the

Cr layer structure from bcc to fcc, as suggested by Brodsky *et al.*<sup>2</sup> [this assumption is supported by the calculation of Xu *et al.*<sup>5</sup> on fcc Cr, with a lattice constant of 3.7 Å, which yields a high  $N(E_F)=2.15$  states/eV], and (2) from their band-theoretical study, Feibelman and Hamann<sup>10</sup> proposed that the high density of interface states at  $E_F$  acts as an effective barrier to reducing the proximity effect and leads to the occurrence of superconductivity.

From the results of our total-energy calculations as a function of lattice spacings, it becomes unrealistic to expect model 1, associated with an anomalously volume expansion (40%) of the Cr lattice, to be correct. This conclusion is consistent with EXAFS measurements<sup>6</sup>, which reveal that Cr atoms in the sample are in a bcc environment. Furthermore, our calculation also confirms the persistence of Cr surface states at the interface as in Ref. 10. More importantly, however, as in Cr(001), these interface states are magnetic in nature with a sizeable magnetic moment of up to  $1.55\mu_B$  for Au/Cr(5- $L$ )/Au(001). This prediction of magnetism is in sharp contrast to the claim of Ref. 10 (i.e., model 2, that the high  $N(E_F)$  of the paramagnetic state is favorable for the occurrence of superconductivity. Based on our spin-polarized and total-energy calculations, we conclude that the superconductivity should be suppressed for Au/Cr/Au(001) sandwiches, due to the strongly magnetic character of the interface states, which leads to magnetic ordering.

Recently, the epitaxy and electronic properties of

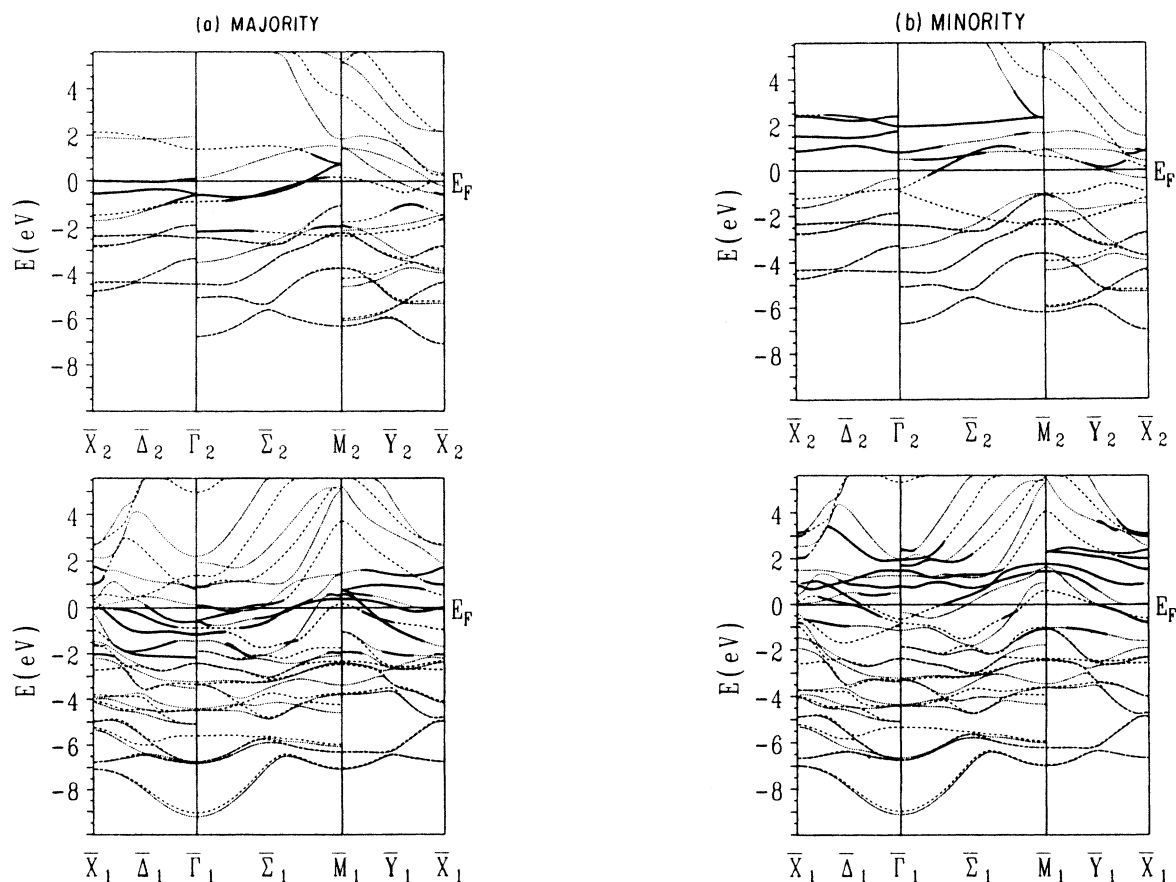


FIG. 6. Energy bands for a seven-layer Au/Cr(3-L)/Au(001) sandwich of a (a) majority spin, and (b) minority spin along high-symmetry directions in the 2D Brillouin zone. Top and lower panels show odd and even symmetries, respectively, with respect to the 2D rotational symmetry. Dashed and dotted lines represent even and odd parities with respect to  $z$  reflection. Solid lines indicate surface states whose wave functions have more than 50% weight within the surface layer.

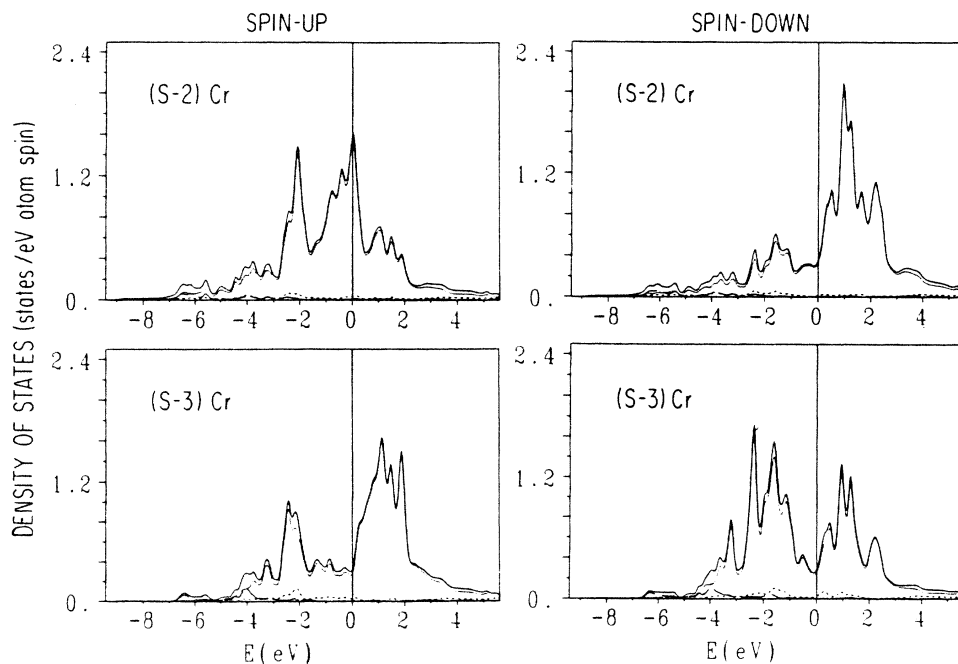


FIG. 7. Layer-projected and  $l$ -decomposed interface and subinterface density of states of the Cr layer in the units of states/(eV spin-atom) for spin-up and spin-down states of a seven-layer Au/Cr(3-L)/Au(001) sandwich.

$p(1 \times 1)\text{Cr}/\text{Au}(001)$  have been studied extensively by Zajac *et al.*,<sup>7</sup> using LEED, Auger, photoemission, and electron-loss spectroscopy. Their results, taken on films prepared at high deposition temperatures (100–150°C) are viewed as favoring a bcc model of Cr—except for the LEED data, which are as consistent with the fcc structure as with the bcc. Furthermore, from the examination of the epitaxy, they conclude that the superconductivity state disappeared once the growth conduction favored epitaxy. In fact, Brodsky *et al.*<sup>2</sup> report the degradation of superconducting properties with time for samples prepared at room temperature in a sample dependent manner: a drop of  $T_c$  with time when the sample was stored at room temperature; however, the observed superconductivity was found to be quite stable if the sample was kept at liquid-nitrogen temperatures. This behavior clearly implies that some sort of annealing from the sample, as prepared to stable or long-term metastable equilibrium structure, takes place. Earlier, superconductivity had been observed in samples of sputter-deposited bcc Cr films,<sup>21</sup> where the superconductivity was attributed to the dilute solution of noble gas in chromium metal (disorder hypothesis). Finally, the apparent disagreement between the x-ray diffraction and EXAFS results is resolved if at most only 10–20% of the sample is fcc, since then the EXAFS would not be able to detect differences from the bcc.<sup>6</sup>

It should also be emphasized that the results obtained do not rely on the thin-slab approximation employed in this investigation. This can be verified from the fact that (i) the work function of our slab is identical to that of the Au(001) surface, and (ii) the magnetic moment of the Cr layer at the center of the slab is very close to bulk Cr for the Au/Cr(5– $L$ )/Au(001) nine-layer film. In fact, our results meet the consistency of an independent band-structure total-energy calculation by Oguchi and Freeman<sup>22</sup> using the linearized muffin-tin orbital method<sup>23</sup> as well as the *bulk* FLAPW method<sup>24</sup> for  $1 \times 1$  and  $3 \times 3$  coherent modulated Au/Cr structures. For the  $3 \times 3$  Au/Cr modulated structure, magnetic moments of  $1.85\mu_B$  and  $-1.05\mu_B$  are found for the interface and subinterface Cr atoms; in addition, there is an induced moment of  $0.08\mu_B$  on the adjacent Au site, and essentially no moment on Au just one-layer beyond the interface. Oguchi and Freeman<sup>22</sup> also find that the Au-Cr alloy with a NaCl structure has a Stoner factor greater than one. These results lend support to the suggestions that the superconductivity is closely tied to disordered Cr.<sup>7</sup>

## V. SUMMARY

We have presented the results of self-consistent, all-electron local-spin-density-functional calculations on Au/Cr/Au(001) sandwiches using the FLAPW total-energy method with a single-slab approach. For the structures thus determined, we find that (i) one layer away from the interface, Cr-bcc and Au-fcc bulk structures are retained, and (ii) the Au-Cr interlayer spacing is very close to the average of the bulk bcc and fcc spacings. We have shown that the basic features of surface states and surface ferromagnetism of Cr(001) are retained (although more delocalized) at the Au/Cr(001) interface. The effect of the Au overlayers decreases the magnetic moment by 0.94 and  $0.5\mu_B$  from the corresponding values of surface and subsurface atoms of the Cr(001) surface. However, a different trend is predicted for the hyperfine contact field of Cr at the interface—the absolute magnitude is *enhanced* by about 50 kG. The inclusion of magnetic other near the interface expands the Au-Cr spacing by 3% from its value in the paramagnetic state. From the agreement with experiment of both the calculated work function and the magnetic moment localized at the center Cr layer, it is concluded that a nine-layer slab [Au/Cr(5– $L$ )/Au(001)] can already give a good quantitative description of the electronic and magnetic properties of even thicker sandwiches (the screening length induced by the interface is of one atomic layer for the charge density and two atomic layers for the spin density).

Models proposed so far to account for the superconductivity were found to be incompatible with results of our total-energy and spin-polarized calculations: we conclude that superconductivity is not a characteristic of the “ordered” Au/Cr interface. Our results are consistent with a recent experimental study of the epitaxy and electronic properties of  $p(1 \times 1)$  Cr/Au(001) as well as an independent calculations on *bulk* modulated Au/Cr layer structures.

## ACKNOWLEDGMENTS

This work was supported by the National Science Foundation (Grant No. DMR-82-16543) and by a grant of computer time from its Office for Advanced Scientific Computing at the University of Minnesota Computing Center. We are grateful to S. D. Bader, M. B. Brodsky, T. Oguchi, and G. Zajac for helpful discussions, and to the University of Minnesota Computing Center for excellent service.

<sup>1</sup>E. Wimmer, H. Krakauer, M. Weinert, and A. J. Freeman, Phys. Rev. B **24**, 864 (1981), and the references therein.

<sup>2</sup>M. B. Brodsky, P. Marikar, R. J. Friddle, L. Singer, and C. H. Sowers, Solid State Commun. **42**, 675 (1982); M. B. Brodsky and H. C. Hamaker, in Superconductivity in *d*- and *f*-Band Metals 1982 (Kernforschungszentrum Karlsruhe, Karlsruhe, 1982), p. 291.

<sup>3</sup>L. E. Klebanoff, S. W. Robey, G. Liu, and D. A. Shirley, Phys. Rev. B **30**, 1048 (1984).

<sup>4</sup>C. L. Fu and A. J. Freeman, Phys. Rev. B **33**, 1755 (1986).

<sup>5</sup>Jian-hua Xu, A. J. Freeman, T. Jarlborg, and M. B. Brodsky,

Phys. Rev. B **29**, 1250 (1984).

<sup>6</sup>S. M. Durbin, L. E. Berman, B. W. Batterman, B. M. Brodsky, and H. C. Hamaker (unpublished).

<sup>7</sup>G. Zajac, S. D. Bader, and R. J. Friddle, Phys. Rev. B **31**, 4947 (1985).

<sup>8</sup>C. L. Fu, A. J. Freeman, E. Wimmer, M. Weinert, Phys. Rev. Lett. **54**, 2261 (1985).

<sup>9</sup>S. Ohnishi, M. Weinert, and A. J. Freeman, Phys. Rev. B **30**, 36 (1984).

<sup>10</sup>P. J. Feibelman and D. R. Hamann, Phys. Rev. B **31**, 1154 (1985).

- <sup>11</sup>M. Weinert, E. Wimmer, and A. J. Freeman, *Phys. Rev. B* **29**, 5267 (1984).
- <sup>12</sup>P. Hohenberg and W. Kohn, *Phys. Rev.* **126**, B864 (1964); W. Kohn and L. J. Sham, *Phys. Rev.* **140**, A1133 (1965).
- <sup>13</sup>M. Weinert, *J. Math. Phys.* **22**, 2433 (1981).
- <sup>14</sup>D. D. Koelling and B. N. Harmon, *J. Phys. C* **10**, 3107 (1977).
- <sup>15</sup>U. von Barth and L. Hedin, *J. Phys. C* **5**, 1629 (1972).
- <sup>16</sup>L. Hedin and B. I. Lundqvist, *J. Phys. C* **4**, 2064 (1971).
- <sup>17</sup>G. Shirane and W. J. Takei, *J. Phys. Soc. Jpn.* **17**, Supp. BIII, 35, (1962).
- <sup>18</sup>C. L. Fu, A. J. Freeman, and T. Oguchi, *Phys. Rev. Lett.* **54**, 2700 (1985).
- <sup>19</sup>H. B. Michaelson, *J. Appl. Phys.* **48**, 4729 (1977).
- <sup>20</sup>A. J. Freeman and R. E. Watson, in *Magnetism*, edited by G. T. Rado and H. Suhl (Academic, New York, 1965), Vol. IIA, p. 67.
- <sup>21</sup>P. H. Schmidt, R. N. Castellano, H. Barg, B. T. Matthias, J. G. Huber, and W. A. Fertig, *Phys. Lett.* **41A**, 367 (1972).
- <sup>22</sup>T. Oguchi and A. J. Freeman, *J. Magn. Magn. Mater.* (to be published).
- <sup>23</sup>O. K. Anderson, *Phys. Rev. B* **12**, 3060 (1975).
- <sup>24</sup>H. J. F. Jansen and A. J. Freeman, *Phys. Rev. B* **30**, 561 (1984).